How the Monomer Concentration of Polymerization Influences Various Properties of Polybenzimidazole: A Case Study with Poly(4,4′-diphenylether-5,5′-bibenzimidazole)

Arindam Sannigrahi, Sandip Ghosh, Joseph Lalnuntluanga, Tushar Jana

School of Chemistry, University of Hyderabad, Hyderabad, India

Received 14 March 2008; accepted 13 August 2008
DOI 10.1002/app.29234
Published online 11 November 2008 in Wiley InterScience (www.interscience.wiley.com).

ABSTRACT: In this work, a series of poly(4,4′-diphenylether-5,5′-bibenzimidazole)s (OPBIs) were synthesized from 4,4′-oxybis(benzoic acid) and 3,3′,4,4′-tetraaminobiphenyl through the variation of the initial monomer concentration with a solution polycondensation technique in a poly(phosphoric acid) medium. The resulting polymers were characterized by various techniques such as infrared (IR), nuclear magnetic resonance, dynamic mechanical analysis (DMA), and thermogravimetric analysis. The initial monomer concentration in the polymerization mixture played an important role in controlling the molecular weight of the resulting polymers. A temperature-dependent IR study showed that the free movement of the —NH group of the imidazole ring was blocked by the absorbed moisture. The DMA study showed that the glass-transition temperature (T_g) varied with the molecular weight, and the presence of the ether linkage in the OPBI polymer backbone had a significant influence on T_g. A high-molecular-weight OPBI polymer tended to form a supramolecular organization, which influenced the thermal characteristic of the polymer. Photophysical studies demonstrated the fluorescent characteristics of the OPBI polymers in both solid and solution states. © 2008 Wiley Periodicals, Inc. J Appl Polym Sci 111: 2194–2203, 2009

Key words: membranes; polyelectrolytes; step-growth polymerization

INTRODUCTION

A fuel cell is an electrochemical energy conversion device for the production of efficient, environmentally friendly, and economical power supplies.[1] Polymer electrolyte membrane fuel cells are the most promising alternatives for portable power applications.[2] In recent years, much effort has been focused on developing new and low-cost polymer electrolyte membranes as substitutes for the very expensive sulfonated perfluoropolymers.[3–9] Also, many of these efforts have been focused on how to increase the operating temperature beyond 100°C, which is the main drawback of the Nafion membrane.[5,6,10] Recently, phosphoric acid (PA) doped polybenzimidazole (PBI) membranes have emerged as promising candidates for low-cost and high-performance polymer electrolyte membrane materials for high-temperature polymer electrolyte membrane fuel cells operating above 120°C.[11–15] Large numbers of high-temperature PBI polymer membranes have been synthesized, and their properties have been explored.[11,12,16–22] PBI has excellent thermochemical resistance, fire-retarding capacity, and insulating properties, and it forms good textile fibers.[16] PBI possesses both proton-donor (—NH —) and proton-acceptor (—N=) hydrogen-bonding sites that exhibit specific interactions with polar solvents,[23–26] and it forms miscible blends with a variety of polymers.[27–30] PBI is used for various purposes, especially high-temperature applications, fiber spinning, reverse osmosis membranes, and fluorescence sensors for halide ions.[16,31] A variety of PBI polymers have been synthesized and reported in the literature, such as poly[2,2′-(*m*-phenylene)-5,5′-benzimidazole] (m-PBI), poly(2,5-benzimidazole),[32] pyridine-based PBI,[11] sulfonated PBI,[22] hyperbranched PBI,[33] fluorinated PBI,[18] and naphthalene-based PBI.[34]

PBI polymers are thermomechanically stable heterocyclic polymers, and they have potential for various industrial applications.[16] However, the major hindrance to their efficient use is their processability, and this arises from the poor solubility and infusibility of the polymers. Hence, several attempts have been carried out to improve the solubility, including

Correspondence to: T. Jana (tjsc@uohyd.ernet.in or tjscuoh@gmail.com).

Contract grant sponsor: Department of Science and Technology; contract grant number: SR/FTP/CS-49/2005 (fast track proposal).

Contract grant sponsor: Council of Scientific and Industrial Research (through a junior research fellowship to S.G.).

incorporating a side chain into the polymer backbone and making the polymer with flexible monomer units.[35–37] 4,4′-Oxybis(benzoic acid) (OBA) is an example of a flexible dicarboxylic acid monomer because the two benzoic acid units in this monomer are connected by an ether linkage. Previously, the synthesis of PBI with this monomer was reported.[19,34,38] However, a detailed study of this type of PBI polymer has not been reported so far. In this study, we synthesized a series of poly(4,4′-diphenylether-5,5′-bibenzimidazole) (OPBI) polymers by varying the initial monomer concentration [total amount of 3,3′,4,4′-tetraaminobiphenyl (TAB) and OBA in poly(phosphoric acid) (PPA)] in the polymerization mixture and using PPA as a polycondensation reagent. We studied the effect of the initial monomer concentration on the various molecular properties of the synthesized OPBI polymers. The synthesized polymers were characterized by the determination of the inherent viscosity (IV) as a measurement of the polymer molecular weight and by thermogravimetric analysis (TGA) for the thermal stability. Fourier transforms infrared (FTIR) and proton nuclear magnetic resonance (^{1}H-NMR) spectroscopy techniques were used to establish the polymer structure. Wide-angle X-ray diffraction was carried out to determine the crystalline nature of these polymers. We studied the thermomechanical properties of polymers of various molecular weights with dynamic mechanical analysis (DMA). Finally, we studied the photophysical properties of these polymers in both solution and solid states.

EXPERIMENTAL

Materials

TAB (polymer-grade), OBA, and PPA (115%) were purchased from Aldrich. Dimethylacetamide (DMAc), formic acid (99%), and sulfuric acid (98%) were purchased from Merck (India). The NMR solvent hexadeuterated dimethyl sulfoxide (DMSO-d_6) was also obtained from Merck. All the chemicals were used without further purification.

Polymer synthesis

Equal molar amounts of TAB and OBA were placed in a three-necked, round-bottom flask along with PPA. The reaction mixture was stirred with a mechanical overhead stirrer, and a slow stream of purged nitrogen gas was maintained throughout the reaction. The reaction mixture was placed in an oil bath, and the temperature was controlled with a temperature controller. Typically, polymerization was carried out at 190–220°C for approximately 26 h. The reaction mixture became more viscous and developed a dark brown color at the end of the polymerization. A small amount of the reaction mixture was poured into double-distilled water and isolated as a brown mass. The mass was pulverized, neutralized with sodium bicarbonate, washed thoroughly with water, and finally dried in a vacuum oven for 24 h at 100°C to obtain dry OPBI for further characterization. The reaction scheme of OPBI synthesis is presented in Scheme 1(A). The initial monomer concentration (total amount of TAB and OBA in PPA) in the polymerization reaction mixture was varied by the placement of the required amounts of TAB and OBA in a fixed quantity of PPA.

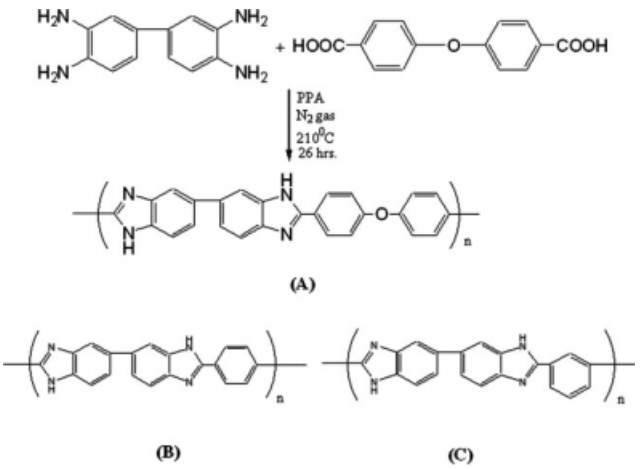

Scheme 1 Syntheses of (A) OPBI, (B) *p*-PBI, and (C) *m*-PBI.

Viscosity

The viscosity of the polymers was measured in H_2SO_4 (98%) solutions at 30°C in a constant-temperature water bath with a Cannon model F725 Ubbelohde capillary dilution viscometer, and the IV values were calculated from the flow time data. The concentration of the polymer solution in H_2SO_4 was 0.2 g/dL for the viscosity measurements.

Infrared (IR) and NMR spectroscopy

The IR spectra of the OPBI films were recorded on a Nicolet 5700 FTIR spectrometer. OPBI films 30–40 μm thick were made from DMAc (2 wt %) solutions. All the NMR spectra were recorded with a Bruker AV 400-MHz NMR spectrometer at room temperature with DMSO-d_6 as an NMR solvent.

Thermal study

Thermogravimetry/differential thermal analysis (TG–DTA) was carried out on a Netzsch STA 409PC TG–DTA instrument from 100 to 900°C at a scanning rate of 10°C/min in the presence of a nitrogen flow.

Before the heating scan, the samples were kept isothermally at 100°C for 20 min inside the TG–DTA furnace.

Mechanical property study

The mechanical properties of the OPBI films were measured with DMA (model Q-800, TA Instruments). OPBI films obtained from DMAc solutions (2 wt %) were boiled repeatedly with distilled water for washing and finally dried in an oven at 100°C for 24 h. Films [25 mm × 5 mm × 0.05 mm (length × width × thickness)] were cut and clamped onto the film tension clamp of the precalibrated instrument. The samples were annealed at 420°C for 10 min, then kept at 100°C isothermally for 20 min inside the DMA machine, and finally scanned from 100 to 430°C at a heating rate of 4°C/min. The storage modulus (E'), loss modulus (E''), and tan δ values were measured at a constant frequency of 10 Hz and a preload force of 0.01 N.

X-ray diffraction

The wide-angle X-ray diffraction patterns of the dry OPBI powders were collected in a Philips model PW 1830 powder diffraction apparatus. The powders were placed on a glass slide, and the diffractograms were recorded with nickel-filtered Cu Kα radiation at a scanning rate of 0.6°/min (2θ).

Photophysical study

Electronic absorption spectra of both the solution and solid were recorded on a Varian Cary-100 Bio ultraviolet–visible spectrometer. Steady-state fluorescence emission spectra of both the solid and solution were recorded on a Jobin Yvon Horiba Fluoromax-3 spectrofluorometer. A dilute OPBI solution in DMAc was prepared, and the solution spectrum was recorded. The dilute OPBI solution in DMAc was spin-coated onto an optically transparent quartz plate, and then the spectrum was recorded from the spin-coated plate.

PA doping level

The dried membranes made from DMAc solutions were immersed into PA (85%) for 7 days and then titrated against NaOH with a Metrohm 702 autotitrator. The PA doping level was calculated as the moles of PA per OPBI repeat unit.

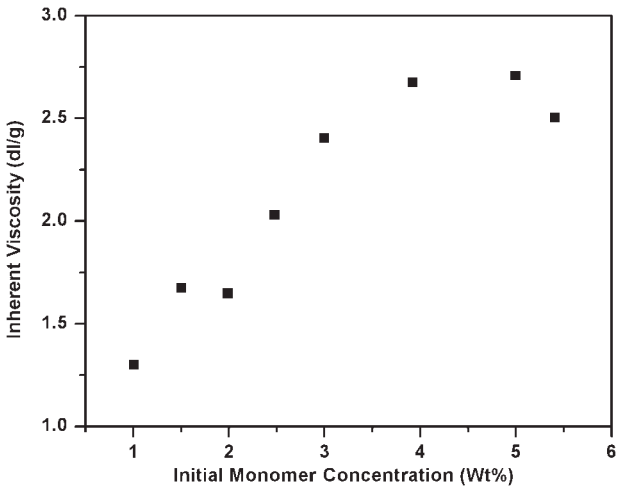

Figure 1 IV of the OPBI polymer versus the initial monomer concentration (total amount of TAB and OBA in PPA) in the polymerization mixtures.

RESULTS AND DISCUSSION

OPBI synthesis and molecular weight

A series of OPBIs of various molecular weights were synthesized with TAB and OBA monomers in a PPA medium at 190–210°C. The initial monomer concentrations (total amount of TAB and OBA in PPA) in the polymerization reaction mixtures were varied from 1 to 5.5% (w/w), and this resulted in a series of OPBI polymers with different molecular weights. A plot of IV against the initial monomer concentration is shown in Figure 1. IV of the polymer solution is a measure of the polymer molecular weight. A higher value of IV indicates a higher molecular weight of the polymer.[39] The quantification of the PBI molecular weight by the measurement of IV in H_2SO_4 has been demonstrated in the literature extensively.[16,38] Figure 1 shows that IV increased with the initial monomer concentration increasing up to 4%, and then IV saturated and finally dropped at a very high initial monomer concentration (5.5%). In a recent article, we have shown that the dicarboxylic acid architecture determines the molecular weights of PBI polymers. Para-structure dicarboxylic acid results in higher molecular weight PBI; we also demonstrated that a relatively low initial monomer concentration is required to obtain a high-IV polymer because of its low solubility in PPA.[17] Because in OBA carboxylic acids are para-structure, we would expect to get a high-IV polymer with a low initial monomer concentration. However, Figure 1 shows the opposite: IV increased with the initial monomer concentration increasing. The presence of the ether linkage in the OBA molecule induced flexibility in OBA, and this resulted in the higher solubility of OBA in PPA. Therefore, more and more OBA molecules were participating in the reaction with the

monomer concentration increasing in the polymerization mixture, and high-IV polymers were yielded. After a certain concentration such as 4% (w/w), IV saturated and then fell, probably because of the supersaturation of OBA molecules in PPA. Hence, from these results, it is clearly evident that the molecular weight of OPBI polymers can be easily tuned through the control of the initial monomer concentration in the polymerization mixture. Another notable observation from this result is that the solubility of dicarboxylic acid plays a vital role in the PBI polymerization, and this observation is in good agreement with our earlier results.[17]

IR and NMR studies

FTIR measurements of OPBI films approximately 30 μm thick were performed with an FTIR spectrometer, and a representative spectrum is shown in Figure 2. The thin films of the OPBI polymers were prepared from dilute solutions of the polymers in DMAc. The films were boiled in hot water thoroughly and dried in a vacuum oven at 100°C for 2 days before the recording of the IR spectra. The absence of C—H stretching of —CH_3 at 2940 cm^{-1} due to DMAC in Figure 2 proves the efficiency of the drying process. The presence of O—H stretching of H_2O at 3620 cm^{-1} in the spectrum is due to the moisture in the film absorbed during the sample handling process. FTIR spectra of PBI polymers were widely discussed earlier by several authors.[20,30,40] The spectrum in Figure 2 shows similar types of bands that have been discussed earlier. The characteristic transmission band around 3415 cm^{-1} due to the N—H stretching frequency of the free —NH groups, the broad transmission at 3148 cm^{-1} due to hydrogen-bonded NH groups, and a low intense peak at 3064 cm^{-1} have been assigned to the stretching frequency of aromatic C—H groups.

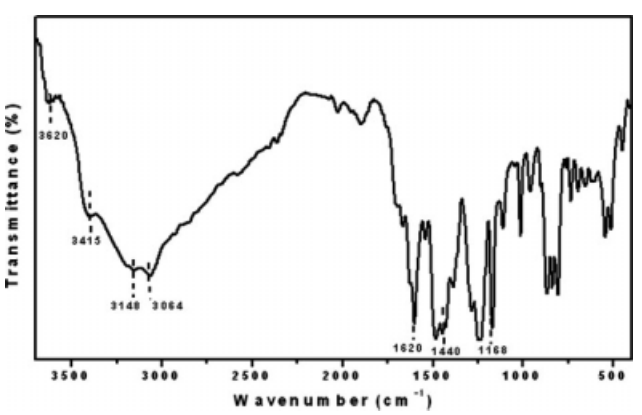

Figure 2 IR spectrum of an OPBI film (thickness ~ 30 μm) made from a DMAc solution. IV of this OPBI polymer was 2.40 dL/g.

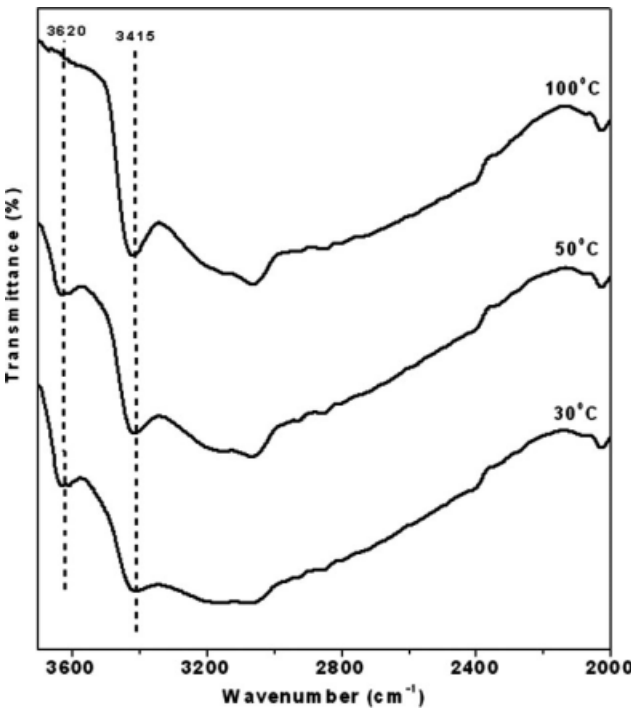

Figure 3 IR spectra of an OPBI (IV = 2.40 dL/g) film (thickness ~ 30 μm) at various temperatures.

The C=C/C=N stretching vibration can be observed at 1620 cm^{-1}. The band around 1440 cm^{-1} belongs to the in-plane deformation of 2,6-disubstituted benzimidazole rings. The peak at 1168 cm^{-1} has been assigned to the ether linkage of OPBI.[41] Figure 3 shows the IR spectra of OPBI films at various temperatures. The OPBI films were kept inside the oven at the indicated temperatures for 2 h, and then IR spectra were immediately recorded with the fast-scan mode. The gradual disappearance of O—H stretching due to absorbed H_2O at 3620 cm^{-1} with increasing temperature is clearly visible in Figure 3. The free N—H stretching band at 3415 cm^{-1} became more intense at a higher temperature. This observation indicates that the water molecules must have hydrated the —NH moiety of the imidazole ring with some kind of weak force, such as hydrogen bonding, at a lower temperature. This possible weak force broke down as the temperature increased because the water molecules evaporated. Therefore, at a higher temperature, the —NH group stretched freely, and this resulted in an intense peak at 3415 cm^{-1}.

Figure 4 shows the ^{1}H-NMR spectrum of OPBI in DMSO-d_6 along with the structure of OPBI and the peak assignment. The assigned peaks in Figure 4 are in good agreement with the anticipated chemical structure. The imidazole peak can be observed at 13.2 ppm, and all the aromatic protons are at 7–8.5 ppm. The large downfield shift of the imidazole

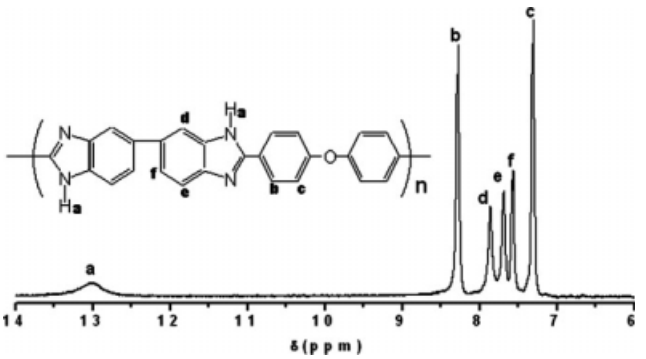

Figure 4 ^{1}H-NMR spectrum of OPBI (IV = 1.67 dL/g) in DMSO-d_6.

proton is due to the hydrogen bonding of the —NH group with the sulfoxide group of the NMR solvent (DMSO-d_6).[25,42]

Thermal stability

The thermal stability of the synthesized OPBI samples was measured in TG–DTA. In all cases, we observed approximately 5% weight loss in the isothermal scan at 100°C. This first weight loss was associated with the loss of loosely bound absorbed water molecules. The samples were subjected to exhaustive drying in a vacuum oven at 100°C before the TGA and IR experiments. Despite this thorough drying process, we observed the weight loss due to absorbed water in TGA and O—H stretching for water molecules in IR (Fig. 2). We also noticed that the O—H stretching frequency of the water molecules decreased with increasing temperature (Fig. 3), and it vanished at 100°C. These observations show that OPBI absorbs moisture readily from the atmosphere and can even absorb moisture during the sample handling time. The TGA curves of OPBI samples

TABLE I
Thermal Stability Data for All the OPBI Polymers

IV	$W_{510°C}$ (%)[a]	$T_{10\%}$[b]	$W_{890°C}$ (%)[c]
1.67	88.95	484.00	66.78
2.03	94.20	584.29	73.82
2.40	93.86	609.10	79.78
2.67	95.02	614.27	79.55
2.70	94.80	619.03	80.69

[a] Residual weight percentage at 510°C.
[b] Temperature at which 10% weight loss is observed.
[c] Residual weight percentage at 890°C.

of different IVs are shown in Figure 5. A distinct weight loss can be observed (Fig. 5) around 510–530°C for all the samples. This second weight loss was due to the degradation of the polymer backbone, which started at a temperature greater than 510°C. Less than 10% weight loss (Table I) was observed at 510°C, and this indicated the remarkable thermal stability of the OPBI polymers. The thermal stability of the OPBI polymer increased with the molecular weight (IV) of the polymer increasing (Fig. 5 and Table I). Table I shows that the temperature at which the 10% weight loss was observed increased with increasing molecular weight (IV), and the weight loss at the final temperature (890°C) became less for the higher molecular weight polymer. The enhancement of the thermal stability for the high-IV polymer occurred because the bigger molecule (polymer chain) needed a higher temperature to degrade. Also, higher IV polymers may have crosslinking that influences the thermal stability.

Interestingly, we have observed that the OPBI polymers were less thermally stable (Fig. 6) than the para-structure PBI, poly[4,4′-(*p*-phenylene)-5,5′-bibenzimidazole] (*p*-PBI). The thermal stability data for *p*-PBI (IV = 2.16 dL/g) were higher (residual

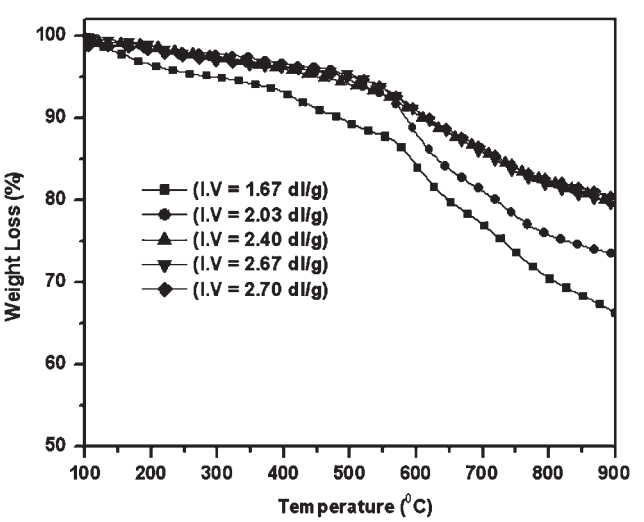

Figure 5 TGA curves of OPBI polymers of various IVs.

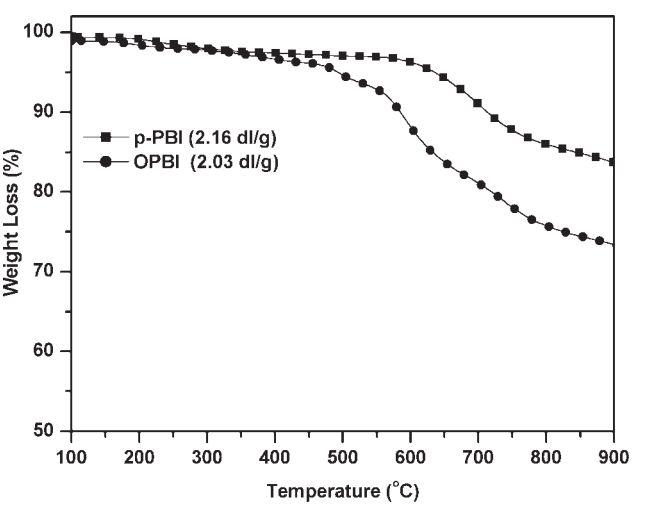

Figure 6 TGA curves of OPBI (IV = 2.03 dL/g) and *p*-PBI (IV = 2.16 dL/g).

weight percentage at 510°C = 97.25, temperature at which 10% weight loss was observed = 709.07, residual weight percentage at 890°C = 84.09) in comparison with OPBI (IV = 2.03 dL/g; Table I). This observation suggests that the incorporation of an ether linkage into the polymer backbone leads to a polymer of lower thermal stability. This is due to the enhancement of the flexibility of the polymer chains from the ether linkages.

Thermal transitions and mechanical properties of OPBI

The thermal transition of a polymer from a glassy state to a rubbery state is recognized by the glass-transition temperature (T_g); in other words, T_g is related to the freezing of the segmental motions of polymer chains.[43] DMA is the most reliable and efficient technique for determining T_g of PBI polymers. The T_g values of all the OPBI and *p*-PBI polymer samples were measured with DMA. The pre-annealing method for DMA scanning was chosen to eliminate the various unidentified, less intense transitions that arose during the first heating run with unannealed samples. Earlier studies on PBI blend system showed that the first DMA heating run results in a complicated structure because of the involvement of various processes such as removal of the residual solvent, glass transitions, and phase separation.[44] Also, it has been proved by IR and TGA studies (discussed earlier) that OPBI is very hygroscopic in nature and can easily absorb approximately 5% (by weight) moisture from the atmosphere. The absorbed moisture may affect the mechanical properties and hence T_g. Therefore, we chose the aforementioned method and could set reproducible T_g values from the DMA study. The T_g values of OPBI and *p*-PBI were 330–352 and 370–382°C, respectively (Fig. 7). The T_g values obtained from the tan δ–temperature plot were 10–20° more than those from the E''–temperature plot. Several authors have reported similar kinds of differences in T_g measurements from E'' and tan δ for various systems.[20,44,45] Hence, T_g of OPBI was 30–40°C lower than that of *p*-PBI as observed from both E'' and tan δ plots of the DMA study (Fig. 7). OPBI (2.03 dL/g) and *p*-PBI (2.16 dL/g) samples of similar IVs were used for the experiments. This means that the difference in T_g between OPBI and *p*-PBI is due to their structural differences. The incorporation of the ether linkage into the OPBI backbone significantly improves the bond rotation probability of the chain. This enhances the flexibility of the polymer chains and thus reduces the glass transition of OPBI in comparison with *p*-PBI. Figure 8 compares E' values of OPBI and *p*-PBI. In both cases, it decreased slightly with increasing temperature, providing evidence for the high thermomechanical stability of the PBI polymers. From Figure 8, it is clear that E' of OPBI is always less than that of *p*-PBI, especially at high temperatures, and this suggests that OPBI has inferior mechanical properties in comparison with *p*-PBI. The enhanced flexibility of the OPBI chains due to the ether linkage could be the answer to the poor mechanical properties in comparison with *p*-PBI.

Temperature-dependent plots of E', E'', and tan δ for all the OPBI membranes are presented in Figure 9(A–C). The high E' values of all the prepared membranes justify the rigid backbone of the OPBI polymers. The E'–temperature plot in Figure 9(A) clearly indicates the presence of significant differences in the mechanical properties with the molecular weight of the polymer increasing. In all cases, E' decreased with increasing temperature, with a little shoulder

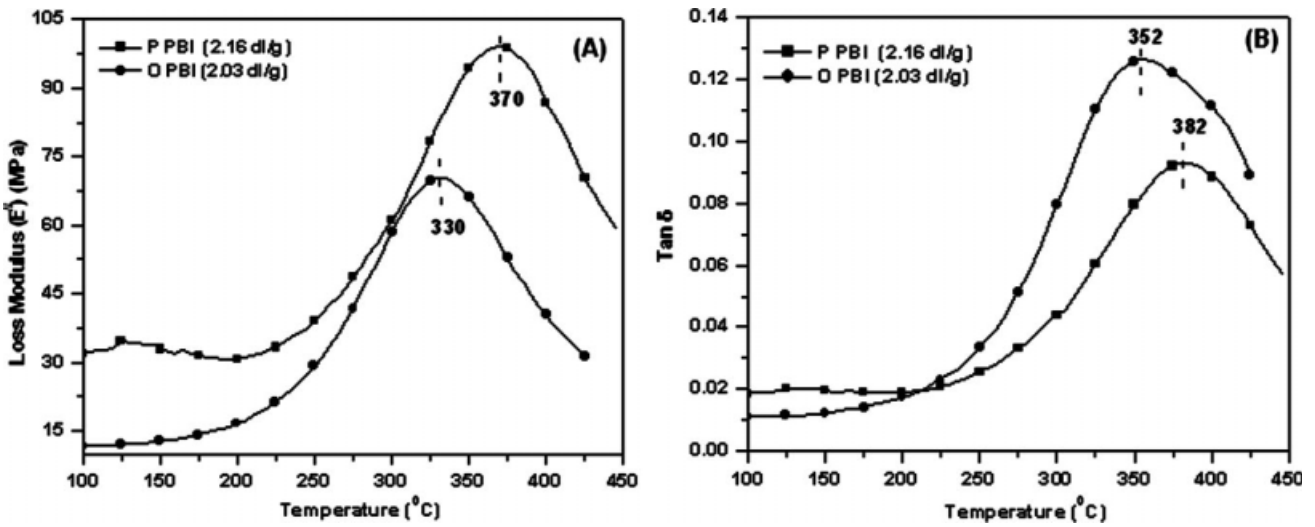

Figure 7 T_g of OPBI (IV = 2.03 dL/g) and *p*-PBI (IV = 2.16 dL/g): (A) E'' versus temperature and (B) tan δ versus temperature (from the DMA study).

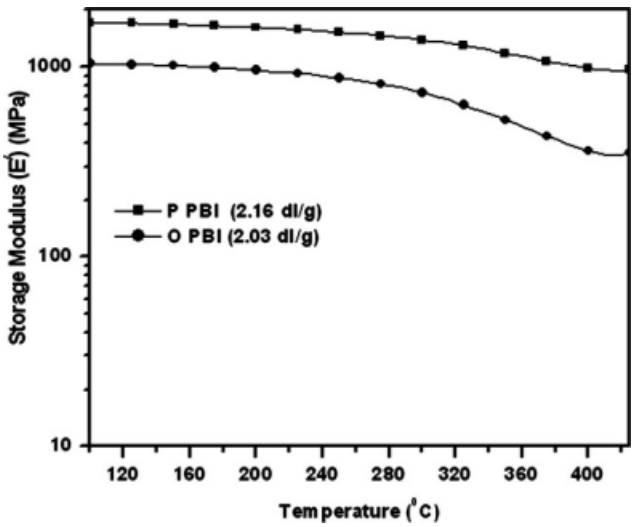

Figure 8 Comparison of mechanical properties (e.g., E') of OPBI (IV = 2.03 dL/g) and *p*-PBI (IV = 2.16 dL/g) films made from DMAc.

near T_g. However, the decrease in E' was very low with increasing temperature. E' had a very high value even at 400°C [Fig. 9(A)], indicating the high thermomechanical stability of the OPBI polymers. A careful analysis of Figure 9(A) reveals that the mechanical property depends on the IV values of the OPBI samples. Table II compares the E' values of OPBI samples of various IVs at different temperature. From Figure 9(A) and Table II, it is clear that the bigger polymer chain (higher IV) had superior mechanical properties. The temperature at which the maximum in E'' and tan δ plots was observed corresponded to the T_g value of the respective OPBI polymer.[43] Figure 9(B,C) shows T_g values for representative OPBI samples of various IVs. T_g of the polymer is closely related to the flexibility of the polymer chains, and a high value of T_g essentially means a high barrier of bond rotations. The energy barrier of bond rotation depends not only on the type of bond but also on the supramolecular organizations of the polymer chains.[46] We observed that T_g

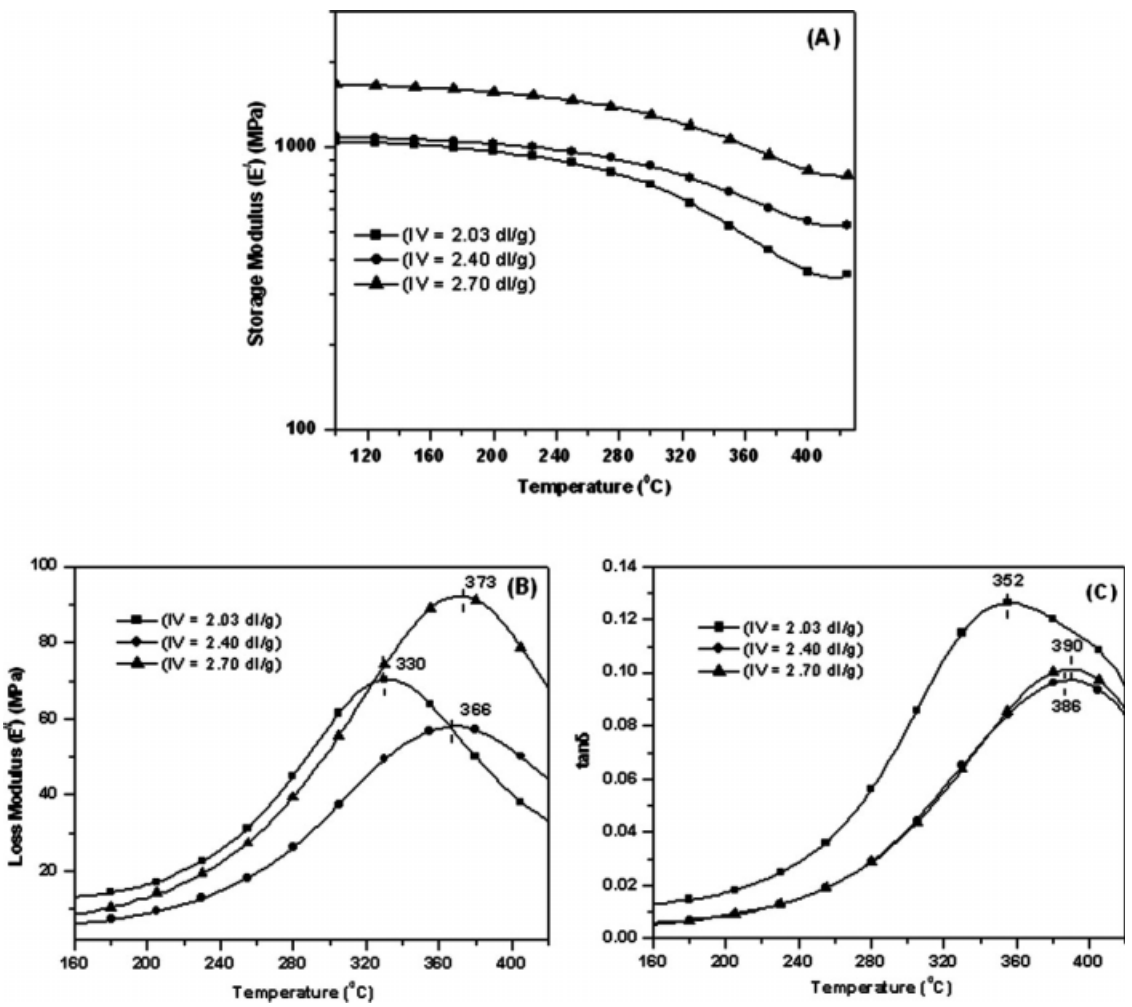

Figure 9 Temperature-dependent plot of mechanical properties obtained from DMA studies of OPBI samples of different IVs: (A) E', (B) E'', and (C) tan δ.

TABLE II
Various Thermomechanical Data for OPBI Films Obtained from the DMA Study

IV (dL/g)	E' (MPa) at 100°C	E' (MPa) at 300°C	E' (MPa) at 420°C
2.03	1046.20	735.69	345.94
2.40	1100.17	855.52	530.51
2.70	1645.24	1295.57	783.43

increased with the increasing molecular weight (IV) of the OPBI polymer [Fig. 9(B,C)]. Hence, we can conclude that with the increasing molecular weight (IV) of OPBI polymers, the polymer chains start overlapping very easily, and this produces bigger supramolecular organization, which leads to an increase in T_g of the OPBI polymers.

X-ray diffraction

Wide-angle X-ray diffraction patterns of representative OPBI samples are presented in Figure 10. From the figure, it is evident that all the samples were amorphous in nature. In all cases, two broad peaks around 11.5 and 21.3° (2θ) were observed. The existence of the broad peaks resulted from a convolution of amorphous and crystalline scattering. Earlier, several authors reported similar observations for PBI-type polymers.[17,34,36,47] However, no sharp peak was observed in any of the cases. Therefore, we can conclude that the molecular weight does not influence the packing capacity of the polymer chains. All the polymers studied here were completely noncrystalline, and so we did not observe any crystalline melting. We obtained a single T_g because of the amorphous nature of the polymers.

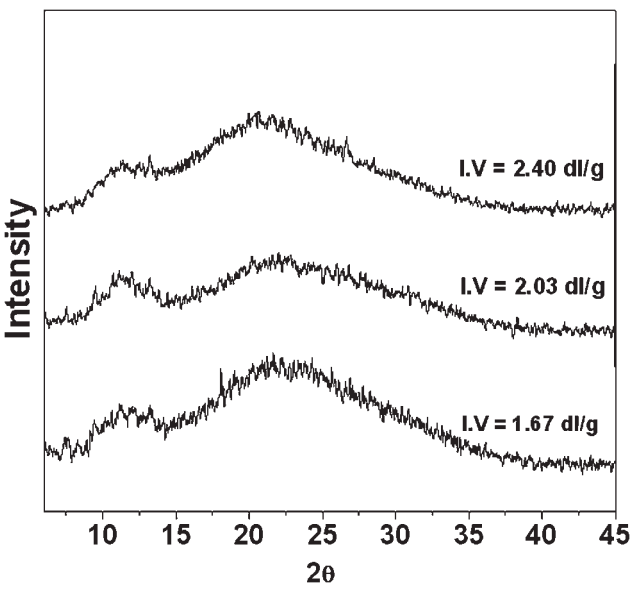

Figure 10 Wide-angle X-ray diffraction patterns of OPBI samples of various IVs.

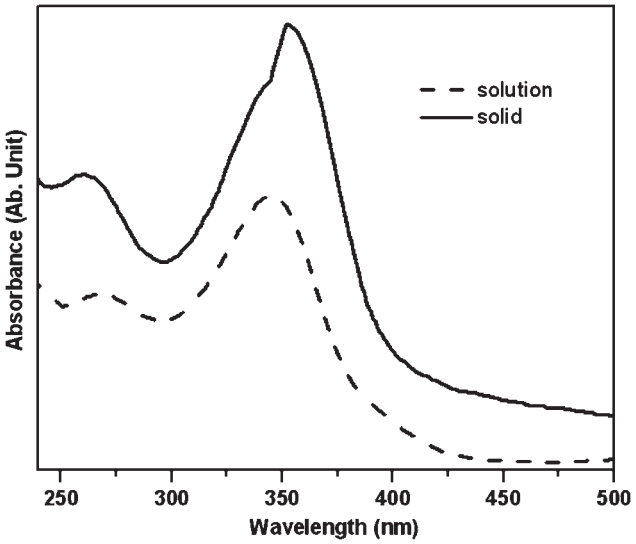

Figure 11 Absorption spectra of OPBI in a DMAc solution and in the solid state.

Photophysical studies

The absorption and fluorescence emission spectra of OPBI samples were studied from dilute solutions in DMAc and in the solid state. To our knowledge, until now no efforts have been made to study the photophysical behavior of PBI-type polymers in the solid state. The electronic absorption spectra of both the solid and solution are presented in Figure 11. Both spectra show two distinct peaks: a lower wavelength peak around 260 nm and higher wavelength absorption around 345 nm. The absorption maxima at $\sim$ 345 nm correspond to the π–π* transition peak of the PBI polymers.[17,25] The OPBI polymer showed identical absorption behavior in both the solid and solution states (Fig. 11).

Figure 12 shows the steady-state emission spectra of OPBI in a DMAc solution and in the solid state. The excitation wavelength was chosen on the basis of the π–π* absorption maxima (λ_{max}) in Figure 11. We recorded the emission spectra (Fig. 12) of both the DMAc solution and the solid state with exactly identical optical densities of these samples at their respective λ_{max} wavelengths. The solution spectrum in Figure 12 shows two closely located emission bands at 390 and 410 nm. Earlier, these peaks were assigned to the 0–0 and 0–1 transitions from the excited ^1L_b state of the benzimidazole ring of the PBI molecules.[17,23,25] The nature and shapes of OPBI in the DMAc solution spectrum are consistent with the earlier reports. The emission band of the solid spectrum is slightly redshifted, and a single broad band can be observed. The most notable feature in

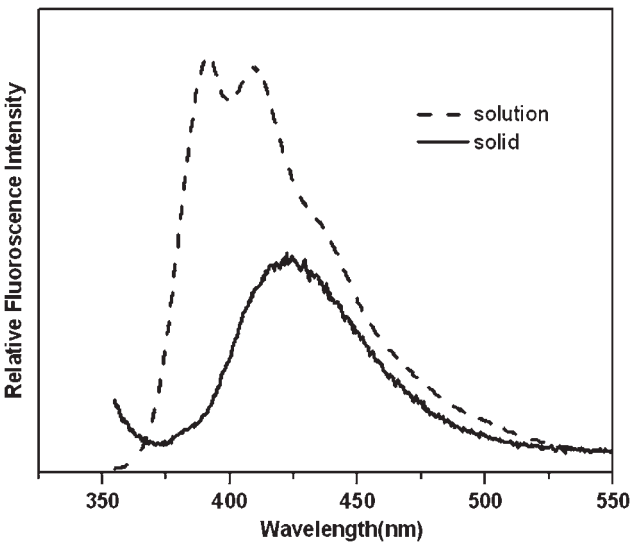

Figure 12 Fluorescence emission spectra of OPBI in a DMAc solution (excitation wavelength = 345 nm) and in the solid state (excitation wavelength = 350 nm).

Figure 12 is the difference in the fluorescence intensity between the solid and solution spectra. Figure 12 shows that the solution fluorescence was much stronger than that of the solid state. The broad emission band and weak fluorescence of the solid OPBI sample demonstrated the existence of the perturbed vibrational relaxation process in the case of the solid OPBI sample.

PA loading

The PA loading capacity of a membrane has a significant influence on the performance of the polymer electrolyte membrane fuel cell. Typically, better cell efficiency is expected with a high PA loading.[11,12] A higher acid content facilitates the transport of the protons, and this significantly improves the fuel cell efficiency.[11,12] The PA doping level of the membrane is expressed as the moles of PA per PBI repeat unit. A large number of efforts have been made to improve the PA doping level of *m*-PBI. Benicewicz et al.[11,12] showed that the PA doping level can be significantly increased by direct casting from the polymerization mixture in PPA. Earlier, we reported that an *m*-PBI membrane made from an *m*-PBI gel in PA showed a very high PA doping level (35–40 mol of PA per PBI repeat unit).[26] The doping level also depends on the molecular weight of OPBI.[12] However, there is no report in the literature on the PA doping level of OPBI. Therefore, we made an effort to study the effect of the molecular weight on the PA loading of OPBI membranes. We prepared an OPBI film from a DMAc solution and then washed it with hot water and kept it in a vacuum oven at 120°C for 24 h. The dried membrane was dipped in 85% PA for 7 days. After that, the PA-doped OPBI film was titrated against 0.1*N* NaOH solutions. The film prepared from the DMAc solution held 4–5 mol of PA per repeat unit, and this did not depend on the IV of the polymer. Unfortunately, the PA loading is too low, and we are currently working on this problem.

CONCLUSIONS

We synthesized and characterized a series of OPBIs consisting of an ether linkage in the polymer backbone by changing the initial monomer concentration in the polymerization reaction mixture. Higher molecular weight polymers were obtained from a higher initial monomer concentration in the polymerization reaction mixture. The thermal stability of the dry polymer powders increased with the molecular weight (IV) of the polymer increasing. The incorporation of an ether linkage into the polymer backbone enhanced the flexibility of the backbone, which influenced the various thermal and thermomechanical properties of this type of PBI (OPBI) in comparison with other PBIs. The OPBI polymer membranes showed excellent thermomechanical stability. T_g increased with increasing molecular weight (IV). All the OPBI polymers synthesized here were completely amorphous in nature. Photophysical studies were carried out both in DMAc solutions and in the solid state. In summary, we conclude that the molecular weight, thermal stability, T_g, and other thermomechanical properties of OPBI polymers can be efficiently controlled by the variation of the initial monomer concentration in the polymerization mixture.

References

1. Fuel Cell Handbook, 6th ed.; EG&G Technical Services: Gaithersburg, MD, 2002.
2. Blomen, L. J. M. J. Fuel Cell Systems; Plenum: New York, 1993.
3. Hickner, M. A.; Ghassemi, H.; Kim, S. Y.; Einsla, B. R.; McGrath, J. E. Chem Rev 2004, 104, 4587.
4. Kerres, J. J Membr Sci 2001, 185, 3.
5. Gottesfeld, S.; Pafford, J. J Electrochem Soc 1998, 135, 2651.
6. Yang, C.; Costamagna, P.; Srinivasan, S.; Benziger, J.; Bocarsly, A. B. J Power Sources 2001, 103, 1.
7. Savadogo, O. J. New Mater Electrochem Syst 1998, 1, 47.
8. Roziere, J.; Jones, D. J. Annu Rev Mater Res 2003, 33, 503.
9. Saxena, A.; Tripathi, B. P.; Shahi, V. K. J Phys Chem B 2007, 111, 12454.
10. Cho, C. G.; Kim, Y. S.; Yu, X.; Hill, M.; McGrath, J. E. J Polym Sci Part A: Polym Chem 2006, 44, 6007.
11. Xiao, L.; Zhang, H.; Jana, T.; Scanlon, E.; Chen, R.; Choe, E. W.; Ramanathan, L. S.; Yu, S.; Benicewicz, B. C. Fuel Cells 2005, 5, 287.
12. Xiao, L.; Zhang, H.; Scanlon, E.; Ramanathan, L. S.; Choe, E. W.; Rogers, D.; Apple, T.; Benicewicz, B. C. Chem Mater 2005, 17, 5328.

13. Savinell, R.; Yeager, E.; Tryk, D.; Landau, U.; Wainright, J.; Weng, D.; Lux, K.; Litt, M.; Rogers, C. J Electrochem Soc 1994, 141, L46.
14. Samms, S. R.; Wsmus, S.; Savinell, R. F. J Electrochem Soc 1996, 143, 1225.
15. Weng, D.; Wainright, J. S.; Landau, U.; Savinell, R. F. J Electrochem Soc 1996, 143, 1260.
16. Choe, E. W.; Choe, D. D. In Polymeric Materials Encyclopedia; Salamone, J. C., Ed.; CRC: New York, 1996.
17. Sannigrahi, A.; Arunbabu, D.; Sankar, R. M.; Jana, T. J Phys Chem B 2007, 111, 12124.
18. Chuang, S. W.; Hsu, S. L. C. J Polym Sci Part A: Polym Chem 2006, 44, 4508.
19. Xu, H.; Chen, K.; Guo, X.; Fang, J. Polymer 2007, 48, 5541.
20. Qing, S.; Huang, W.; Yan, D. Eur Polym J 2005, 41, 1589.
21. Osaheni, J. A.; Jenekhe, S. A. Macromolecules 1995, 28, 1172.
22. Jouanneau, J.; Mercier, R.; Gonon, L.; Gebel, G. Macromolecules 2007, 40, 983.
23. Kojima, T. J Polym Sci Polym Phys Ed 1980, 18, 1685.
24. Shogbon, C. B.; Brousseau, J. L.; Zhang, H.; Benicewicz, B. C.; Akpalu, Y. Macromolecules 2006, 39, 9409.
25. Sannigrahi, A.; Arunbabu, D.; Sankar, R. M.; Jana, T. Macromolecules 2007, 40, 2844.
26. Sannigrahi, A.; Arunbabu, D.; Jana, T. Macromol Rapid Commun 2006, 27, 1962.
27. Musto, P.; Karasz, F. E.; MacKnight, W. J. Macromolecules 1991, 24, 4762.
28. Deimede, V.; Voyiatzis, G. A.; Kallitsis, J. K.; Qingfeng, L.; Bjerrum, N. J. Macromolecules 2000, 33, 7609.
29. Wang, Y.; Goh, S. H.; Chung, T. S. Polymer 2007, 48, 2901.
30. Musto, P.; Karasz, F. E.; MacKnight, W. J. Polymer 1993, 34, 2934.
31. Yang, N. C.; Sang, M. L.; Suh, D. H. Polym Bull 2003, 49, 371.
32. Asensio, J. N.; Borrós, S.; Gómez-Romero, P. J Electrochem Soc A 2004, 151, 304.
33. Li, Z. X.; Liu, J. H.; Yang, S. Y.; Huang, S. H.; Lu, J. D.; Pu, J. L. J Polym Sci Part A: Polym Chem 2006, 44, 5729.
34. Chen, C. C.; Wang, L. F.; Wang, J. J.; Hsu, T. C.; Chen, C. F. J Mater Sci 2002, 37, 4109.
35. Pu, H.; Liu, Q.; Liu, G. J Membr Sci 2004, 241, 169.
36. Scariah, K. J.; Krishnamurthy, V. N.; Rao, K. V. C.; Srinivasan, M. J Polym Sci Part A: Polym Chem 1987, 25, 2675.
37. Persson, J. C.; Jannasch, P. Chem Mater 2006, 18, 3096.
38. Neuse, E. W. Adv Polym Sci 1982, 47, 1.
39. Sun, S. F. Physical Chemistry of Macromolecules: Basic Principles and Issues; Wiley: New York, 1994.
40. Lobato, J.; Cañizares, P.; Rodrigo, M. A.; Linares, J. J.; Manjavacas, G. J Membr Sci 2006, 280, 351.
41. Silverstein, R. M.; Webster, F. X. Spectroscopic Identification of Organic Compounds; Wiley: New York, 2002.
42. Kojima, T. J Polym Sci Polym Phys Ed 1980, 18, 1673.
43. Sperling, L. H. Introduction to Physical Polymer Science; Wiley: New York, 1992.
44. Liang, K.; Bánhegyi, G.; Karasz, F. E.; MacKnight, W. J. J Polym Sci Part B: Polym Phys 1991, 29, 649.
45. Manna, S.; Batabyal, S. K.; Nandi, A. K. J Phys Chem B 2006, 110, 12318.
46. Fernández-Blázquez, J. P.; Bello, A.; Pérez, E. Polymer 2005, 46, 10004.
47. Kumbharkaar, S. C.; Karadkar, P. B.; Kharul, U. K. J Membr Sci 2006, 286, 161.